Biomass Leachate Treatment and Nutrient Recovery Using Reverse Osmosis: Experimental Study and Hybrid Artificial Neural Network Modeling

ARTICLE *in* ENERGY & FUELS · DECEMBER 2012

Impact Factor: 2.79 · DOI: 10.1021/ef301452s

4 AUTHORS, INCLUDING:

Amin Reza Rajabzadeh
McMaster University
20 PUBLICATIONS **42** CITATIONS

SEE PROFILE

energy&fuels

Article

pubs.acs.org/EF

Biomass Leachate Treatment and Nutrient Recovery Using Reverse Osmosis: Experimental Study and Hybrid Artificial Neural Network Modeling

Amin Reza Rajabzadeh,* Nick Ruzich, Sohrab Zendehboudi, and Mohammad Rahbari

CENNATEK, Incorporated, 1086 Modeland Road, Building 1010, Sarnia, Ontario N7S 6L2, Canada

ABSTRACT: The application of reverse osmosis (RO) to recover nutrients from biomass leachate, with special reference to permeate flux behavior during the filtration of the leachate, is investigated in this paper through a comprehensive laboratory and modeling approach. Various sources of biomass, including soybean straw, switchgrass, and miscanthus, were industrially leached using distilled water with agitation during the extraction experiments. The leachates were filtered using a RO flat sheet membrane module to recover the nutrients and water. On the basis of inductively coupled plasma (ICP) analytical results, calcium, magnesium, phosphorus, and silica for all types of biomass leachate samples had rejection efficiencies of >80%. Permeate flux decreased sharply at the beginning of the filtration, followed by a slight decline during the filtration process. A hybrid intelligent model based on a feed-forward artificial neural network (ANN) was also developed to estimate the permeate flux during the filtration in terms of the filtration time and total solid concentration in the leachate. A Levenberg−Marquardt optimization algorithm was chosen to perform the training phase for the network. An ANN with four neurons in one hidden layer was selected as the optimum structure, such that a maximum percent absolute error of 14% was attained while predicting the permeate flux. A reasonable agreement was observed between the ANN predictions and experimental data, which exhibits the potential usefulness of the hybrid ANN model to predict permeate flux during RO filtration of biomass leachate.

1. INTRODUCTION

Biomass is considered a renewable energy source capable of providing a small portion of the world's steadily growing energy demand currently being supplied mostly by fossil fuels especially in the Organisation for Economic Co-operation and Development (OECD) countries. According to the Energy Information Administration (EIA),[1] biomass provides a small but growing share of the industrial sector energy basket among the OECD countries, from 7% in 2008 to 10% in 2035. Currently, biomass is responsible for a notable part of the renewable energy consumed in the industrial section. For instance, the use of renewable fuels, such as biomass, is growing faster than any other energy sources in the U.S. industrial section, from 10% in 2008 to 16% in 2035, because of the rising oil prices.

The combustion of biomass is limited because of some undesired process phenomena, such as fouling, slagging, agglomeration of bed media, and corrosion of equipment (e.g., reactors, furnaces, heat exchangers, turbines, and emission control devices).[2−6] These operational issues have led to a significant reduction in efficiency of thermal conversion plants. The main reason for this low efficiency is the presence of alkali metals, phosphorus, chlorine, sulfur, and silica in agricultural biomass.[2,6−9] As a result, combustion properties of biomass can be improved by extracting these nutrients from biomass.[10−14] The majority of inorganic constituents (except silica) in biomass are water-soluble and can be removed through industrial water leaching. The removal of the alkali compounds will result in reduced maintenance costs and higher thermal conversion efficiency.[15]

Yu et al.[14] explored the effectiveness of immersion leaching with agitation on sugar beet pulp. Leaching times of 30 min and 2 h were tested, at water/biomass ratios of 20 and 50 mL g^{-1}. Results indicated that the leachate extracted 70−86% potassium, 70−82% sodium, and 64−76% chlorine from biomass. Arvelakis et al.[16,17] examined the leaching of peach stones and olive oil residue. The biomass was immersed with no agitation at a water/biomass ratio of 15:1 (mL g^{-1}) for 8 h at room temperature. There were relatively lower reductions in the levels of potassium (45%) and chlorine (61%), while aluminum (96%), iron (84%), and sodium (76%) showed larger reductions in the leached material. The olive oil residues (including kernels, pulp, leaves, and limbs) resulted in significant nutrient reductions for sodium (98%), chlorine (97.9%), aluminum (79%), magnesium (75%), and potassium (65%). Giuntoli et al.[18] examined the effect of immersion leaching on the combustion characteristics of wheat straw, peach stones, and olive residue. Water/biomass ratios between 67:1 and 89:1 (mL g^{-1}) and residence times of 23−24 h were examined. All three residues showed a decrease in potassium (31−63% reduction), sodium (71−99% reduction), and chlorine (44−100% reduction). Different leaching operating conditions, such as retention times (6−24 h) and mass/water ratios (75−625 mL g^{-1}), were tested by Arvelakis and Koukios.[19]

One concern associated with the industrial leaching process is the high volume of water required for the extraction process. Typical values of the water/biomass ratio are in the range of 15−120 mL g^{-1} for the leaching process.[13,16−18,20] Thus, use of

Received: September 5, 2012
Revised: November 10, 2012
Published: November 12, 2012

dx.doi.org/10.1021/ef301452s | *Energy Fuels* 2012, 26, 7155−7163

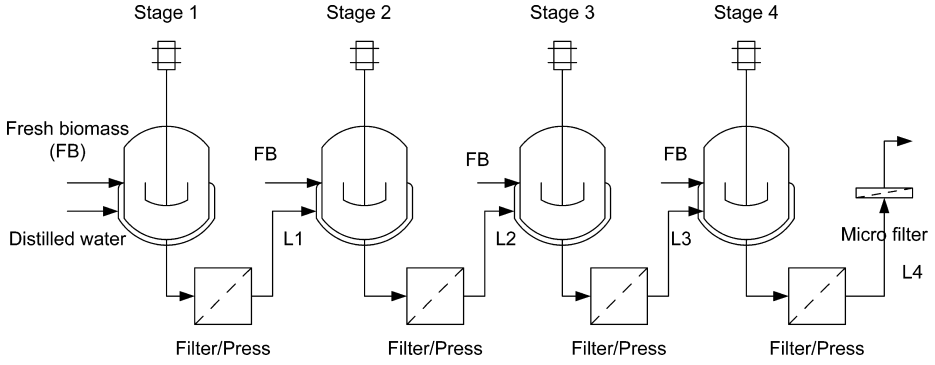

Figure 1. Multi-stage biomass leaching process.

processing technologies is inevitable to recover water consumed in the leaching process facilities.

Reverse osmosis (RO) is a membrane-based filtration technique that has efficient applicability in water recovery. RO is a pressure-driven operation, in which the transmembrane pressure (TMP) provides a driving force for a solvent (water) to permeate through the membrane, while nutrients are retained by the membrane. The permeate stream is free of nutrients and is normally recycled to the leaching facility. The rejected stream from the membrane (retentate), which is rich in nutrients, can be sent back to farms, in the form of a liquid fertilizer, to compensate for the nutrients taken from soil in an efficient manner. Consequently, recycling the nutrients to farms amends the fertility of soil and alleviates the concern of soil nutrient depletion.[21] The RO filtration has various common applications, including desalination of seawater and brackish water, waste treatment for the recovery of metals for finishing industries, and water reclamation of municipal and industrial wastewaters.[22]

Nutrient recovery from aquatic systems using RO membranes has been widely reported in the literature. The possibility of nutrient recovery from an anaerobically treated black water (concentrated stream of decentralized wastewater) using RO technology was studied by Van Voorthuizen et al.[23] Black water was found to be rich in nitrogen (as ammonium) and phosphate. According to their results, rejections for ammonium and phosphate were obtained in the ranges of 80−90 and 90−100%, respectively. Bilstad[24] investigated the feasibility of RO for the separation of nitrogen from domestic wastewater using tubular and spiral-wound membrane modules. A nitrogen separation efficiency of 95% was attained with both membrane modules. It was also found that RO membranes could not operate efficiently with suspended solids. Hence, upstream pretreatments, such as prefiltration stage(s), were needed to remove suspended solids. RO has also been tested for water recovery from leachates obtained by water-washing biomass. Jenkins et al.[10] conducted water leaching of rice straw, followed by RO filtration of the leachate. Rice straw was submerged in deionized water for 24 h at room temperature without agitation (10 kg of biomass/350 L). A spiral-wound module consisting of a low-pressure thin-film (TF) composite membrane (2.42 m^2) was used to filter the leachate. More than 90% of the water was recovered from the leachate, while the ion rejection by the membrane was above 90%. Colyar[25] performed the leaching of wet corn stover using a stirred tank reactor for immersion leaching with agitation. The biomass was placed in a jar filled with water (water/biomass ratio of 4:1, w/w) and was agitated with an overhead stirrer operating at 10−30 rpm. The leachate was filtered via a sequential membrane setup of ultrafiltration (UF) and RO. A total of 100% of the total suspended solids and 10−20% of the soluble total organic carbon (TOC) in the leachate were separated by the UF membrane. High rejections (>70%) of phosphate, potassium, chloride, and TOC species were reported by the RO membrane.

The primary motivation of implementing the present study was to improve our understanding of the permeate flux behavior during the RO filtration of biomass leachate. It also aimed to determine the amount of nutrients recovered from the biomass leachate using the RO process. In this paper, the performance of RO for nutrient recovery through a combined experimental and modeling approach is discussed. Samples of three types of biomass, namely, soybean straw, switchgrass, and miscanthus, were leached using distilled water with agitation. The biomass samples were analyzed for elemental composition prior to leaching. The leachate was concentrated by employing a cross-flow RO membrane filtration system. The permeate flux was measured versus time during the filtration. Leachate, permeate, and retentate streams were analyzed using the inductively coupled plasma−optical emission spectrometry (ICP−OES) technique to obtain the elemental composition. In addition, a hybrid artificial neural network (ANN) system was developed to predict the permeate flux during the RO filtration of biomass leachate. The experimental data were divided into three categories, namely, training, testing, and validation data sets, to be used in building the ANN model.

2. EXPERIMENTAL SECTION

2.1. Biomass Samples. Various biomass feedstocks for lab-scale experiments were obtained from local Ontario producers including: two energy crops (miscanthus and switchgrass) and one agricultural residue (soybean straw). All three biomass samples were harvested in the fall. Prior to the industrial leaching, each biomass was passed through a Wiley knife mill for size reduction (Thomas ED-5 Wiley Mill, Swedesboro, NJ). The reduction in particle size increased the available surface area of the biomass, providing a greater contact area between the water and nutrients in the biomass. In addition, the smaller particles increased the rate of extraction by decreasing the path of diffusion, which is a key factor in the overall rate of extraction. The particle size attained by the knife mill was lower than 2.0 mm. A drying step was applied prior to milling if the moisture content of the raw biomass was above 10%. Biomass with a moisture content above 10% could cause clogging in the knife mill.

2.2. Leaching Procedure. Leaching was carried out using distilled water (resistivity > 18.5 MΩ cm) at a water/biomass ratio of 12:1 (mL g^{-1}). Biomass was immersed in distilled water in a 2 L vessel and agitated using a two-blade flat impeller running at 300 rpm at room temperature for 1 h. The mixture was filtered to produce the liquid

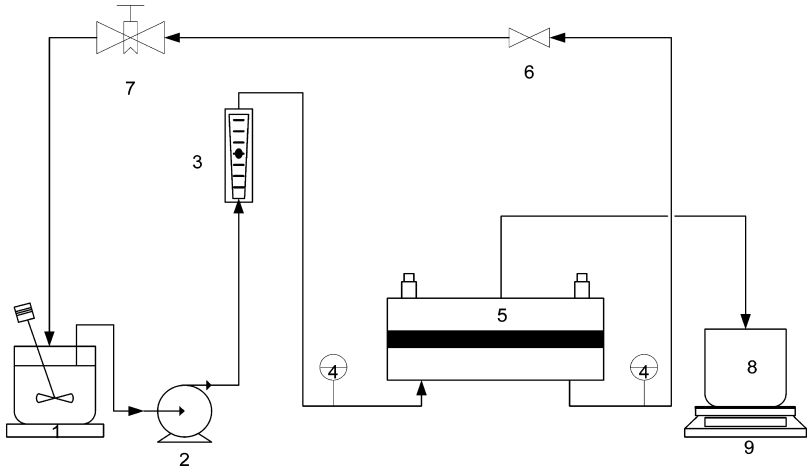

Figure 2. Schematic diagram of the filtration unit: (1) feed tank, (2) pump, (3) flowmeter, (4) pressure gauge, (5) membrane, (6) pinch valve, (7) sampling valve, (8) permeate container, and (9) balance.

extract. The wet biomass was further dewatered using a 10 ton hydraulic press to extract more liquid and to further reduce the moisture content. A portion of the biomass was then dried using an infrared moisture analyzer (Denver Instrument IR-35) prior to analytical tests. The moisture content of biomass after press was about 65%. The leachate was vacuum-filtered with a 1.5 μm filter paper before running the RO trials.

2.2.1. Leaching in Series. Multiple-stage leaching was carried out to reduce the water consumption of the process. A schematic diagram of the process is presented in Figure 1. In stage 1, leaching was performed using distilled water, filtered by a cloth filter bag, and pressed to produce leachate 1 (L1). In all of the other stages, leachate from the previous stage was introduced to fresh biomass (FB). In all four stages, leaching was conducted for 1 h at a liquid/biomass ratio of 12:1 (mL g^{-1}) and at room temperature. Leachate from the last stage (L4) was filtered through 1.5 μm filter paper before the RO trials.

2.3. RO Experimental Setup. The details of the experimental setup are given in Figure 2. Briefly summarized, a lab-scale CF042 cross-flow cell (Sterlitech Corporation, Kent, WA) was used as a membrane module. A rectangular piece of TF composite polyamide RO membrane was placed at the base of the cell. The membrane was manufactured by KOCH Membrane Systems (TFC-HR KMS). Feed entered the cell from the base of the cell into the membrane cavity, where it flowed tangentially across the membrane surface. The effective membrane surface area was about 42 cm^2. The feed was pumped by a diaphragm feed pump [M-03S Hydracell Pump, Viton Diaphragms 1.8 gallons per minute (GPM)], and the flow rate was measured using a site-read panel mount flowmeter (F-55376L, 316SS float material, 0.2−2.0 GPM). Pressure was monitored at the feed and retentate sides with two pressure gauges (Swagelok, 0−100 bar). TMP was controlled on the retentate side by a manual pinch valve. The permeate flow was collected in a reservoir, and its mass was measured using a lab-scale balance. Permeate flux was measured via weighing permeate at specified time intervals. The feed tank was placed in a water bath (Digital Circulator, 6 L, PolyScience, Vernon Hills, IL) to maintain the temperature at 25 °C. A 2 L glass Erlenmeyer flask was used as a feed tank for the experiments. The system holdup was 230 mL.

2.4. Analytical Methods. Solid biomass samples underwent standard characterization testing for use in thermal processes. The tests (summarized in Table 1) include proximate and ultimate analyses, calorific value [or higher heating value (HHV)], chlorine, elemental ash composition, and ash fusion temperatures. The leachates produced in the experiments were also measured for nutrient content using ICP−OES.

Table 1. Characteristics of Untreated Biomass Feedstock and ASTM Test Methods for Analysis of Biomass Samples[a]

parameters	miscanthus	switchgrass	soybean
proximate analysis			
moisture (wt %)	12.64	9.56	7.43
ash (wt % dry matter)	2.66	1.96	2.79
ultimate analysis (% dry matter)			
carbon	46.99	49.32	43.08
hydrogen	5.94	5.89	5.64
nitrogen	0.09	0.28	0.7
sulfur	0.01	0.02	0.02
oxygen[b]	44.31	42.53	47.77
ash fusion (°C)[c]			
initial deformation temperature	916	1227	>1538
softening temperature	1022	1238	>1538
hemispherical temperature	1224	1250	>1538
fluid temperature	1317	1265	>1538
chlorine (wt % dry matter)	0.14	0.1	0.12
calorific value (MJ/kg)	19.12	18.43	17.67
elemental ash composition (% ash)			
SiO_2	61.25	51.69	13.55
P_2O_5	6.75	5.97	8.72
Al_2O_3	0.59	0.98	2.08
Fe_2O_3	0.37	0.65	1.05
MnO	0.3	0.05	0.08
MgO	3.66	9.37	21.5
CaO	6.13	22.67	43.26
K_2O	19.48	8.01	8.74
Na_2O	1.4	0.51	0.87
TiO_2	0.02	0.06	0.1
Cr_2O_3	0.06	0.04	0.05

[a]ASTM test methods: moisture content (wt %), E871; ash content (% dry matter), E1755; carbon, hydrogen, and nitrogen, D5373; sulfur, D4239; oxygen, E870; chlorine, D4208; calorific value (HHV), E711; elemental ash composition, D6349; and ash fusion temperatures (°C), D1857. [b]Calculated by difference. [c]Ash preparation was carried out at 575 °C.

3. MODELING

3.1. ANN. *3.1.1. Principles.* ANN is a mathematical technique that has been recently employed for numerous applications, such as process control, behavior prediction, model recognition, and system classification. An ANN consists

of a number of interconnected processing elements (neurons or nodes) working in parallel to solve complex problems. Figure 3

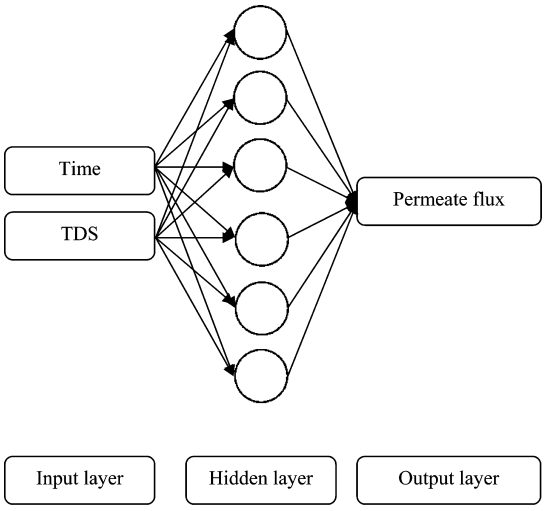

Figure 3. Simple structure of an ANN with one hidden layer.

depicts a typical structure of ANN consisting of an input layer, one hidden layer, and an output layer. Each neuron is connected to the input and output by means of weighted connections. A nonlinear transformation of the weighted sum of the inputs is performed in each neuron to produce the outputs.[26] Initial values of weights are randomly assigned and then modified through a training process until the best fit of predicted outputs is generated. The most widely used training algorithm is known as the back-propagation (BP) method, in which the connection weights are modified from the output layer back to the input layer at each iteration until the mean-squared error (MSE) meets the tolerance specified for the case study. The BP algorithm adjusts the weights using the gradient descent principle, where the change in the weight is along the negative of the error gradient.[27,28] The performance of the ANN model is finally checked by introducing new and independent data sets to the trained model.

3.1.2. Data Processing. The inputs to the proposed ANN model included the filtration time and total solid concentration. The output of the ANN model was the permeate flux. To avoid any false influence of factors with a higher order of magnitude, all model input and output variables were normalized in the range of $(-1, 1)$. Data normalization was performed using eq 1 as follows:

$$X = \frac{x - \frac{(x_{max} + x_{min})}{2}}{\frac{(x_{max} + x_{min})}{2}} \quad (1)$$

where x_{max} and x_{min} are the highest and lowest values of variable x, respectively. The whole experimental data set was composed of 135 permeate fluxes. The ANN model was trained using 95 experimental data points selected randomly from the available data sets. MATLAB software, version 7, from Mathworks, Natick, MA, was employed for the ANN modeling. The Levenberg–Marquardt optimization algorithm was employed as the BP technique for training the neural network. Hyperbolic tangent sigmoid and linear functions were the transfer functions for the hidden and output layers, respectively. The performance of the ANN model was tested and validated by independent and unseen data sets. One hidden layer was selected in the ANN model. According to the universal approximation theory, one hidden layer with a sufficient number of neurons can model any set of input/output data to a reasonable degree of precision.[29]

3.2. Membrane Mathematical Equations. As discussed in section 3.1.2, the total dissolved solids (TDS) concentration is one of the inputs considered for the ANN model. The total solid concentration at a given filtration time depends upon the permeate flux, which is the output of the ANN model. The total solid concentration in the feed tank increases during the filtration as permeate is removed from the feed tank. The change in the feed volume is obtained by writing a mass balance over the feed tank

$$\frac{dV_F}{dt} = -Q_P = -JA \quad (2)$$

where Q_P is the permeate volumetric flow rate, V_F is the feed volume, t is the filtration time, J is the permeate flux, and A is the effective membrane surface area. The feed volume is determined by integrating the permeate flow rate over the filtration time.

The feed tank is modeled as a well-mixed continuous stirred tank. With the well-mixed assumption, the transient solute concentration is uniform in the feed tank. No solute accumulation in the pipeline between the feed tank and the membrane module is assumed. The change of the solute concentration in the feed tank with respect to time is given by eq 3

$$\frac{dC_F}{dt} = \frac{Q_P}{V}(C_F - C_P) \quad (3)$$

where C_F and C_P are the feed and permeate total solid concentrations, respectively. The change rate of the solute concentration in the feed tank depends upon the magnitude of the permeate flow rate and the rejection coefficients of the solutes (R). The rejection coefficient describes the separation efficiency of a RO membrane system by relating the permeate concentration to the feed concentration as follows:

$$R = 1 - \left(\frac{C_P}{C_F}\right) \quad (4)$$

By substituting eq 4 into eq 3 and then rearranging, eq 5 is obtained as follows:

$$\frac{dC_F}{dt} = \frac{Q_P}{V_F}(C_F R) \quad (5)$$

The total solid concentration in the feed tank at a given time is computed by integrating eq 5 over the filtration time.

3.3. ANN Model and Membrane Mathematical Equations. Figure 4 is the schematic representation of the algorithm proposed in this work to predict the permeate flux during the RO filtration of biomass leachate. The algorithm includes the trained ANN model coupled with membrane mathematical equations. The inputs of the algorithm consist of the feed and membrane characteristics. The feed properties are the initial total solid concentration in the feed tank (at time zero) and the initial feed volume. The membrane specifications include the membrane surface area and the rejection coefficient of total solid by the RO membrane. The permeate flux is estimated by the trained ANN model based on the inputs of the model, which are the total solid concentration of the feed

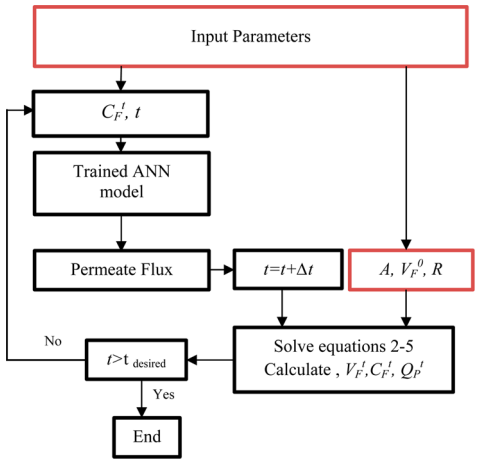

Figure 4. Flow diagram of ANN model coupled with membrane mathematical equations to predict permeate flux.

solution at time zero. The variations in the leachate feed volume and total solid concentration at time $t + \Delta t$ are calculated by integrating eqs 2 and 5 over the filtration time. The new total solid concentration in the feed tank and the filtration time are fed to the ANN model to estimate the new permeate flux for the next time step. The algorithm proceeds until the desired filtration time is reached.

4. RESULTS AND DISCUSSION

4.1. Analysis of Biomass Samples and Leachate.

Miscanthus, switchgrass, and soybean samples were analyzed prior to leaching for moisture and ash contents (proximate analysis), CHNSO (ultimate analysis), chlorine, HHV, ash fusion temperatures, and elemental ash composition. The results are shown in Table 1. Biomass was immersed in water and agitated at room temperature for 1 h. The produced leachate was filtered with a 1.5 μm filter paper and analyzed for the nutrient content using an ICP−OES method (Table 2).

Table 2. Concentration of Nutrients in Leachate after One Leaching Cycle, C_L (mg L^{-1}), and Percent Removal of Nutrients in Biomass, R'' (%)

	miscanthus		switchgrass		soybean	
elements	C_L (mg L^{-1})	R'' (%)	C_L (mg L^{-1})	R'' (%)	C_L (mg L^{-1})	R'' (%)
sodium	7.1	31	1.8	29	5.6	37
calcium	18.5	19	26.7	10	34	5
potassium	187.2	52	79.1	73	85.9	51
magnesium	15	31	35.7	39	59.5	20
phosphorus	41.5	64	16.6	39	22.3	25
chlorine	121.6	100			89.1	89
silica	4.8	1	3.3	1	1.6	1
total solid	2587		2474		1740	

Chlorine and potassium were the most leachable nutrients in biomass. Approximately 100% of chlorine in miscanthus was extracted into leachate. Chlorine extraction from soybean straw into leachate was 89%. Extraction of potassium from miscanthus, switchgrass, and soybean samples was around 52, 73, and 51%, respectively. The extraction efficiency was calculated by dividing the absolute mass of elements in leachate by those in dry biomass. Other elements with moderate extractions were magnesium, phosphorus, sodium, and to a lesser amount, calcium. Only 19, 10, and 5% of calcium in miscanthus, switchgrass, and soybean were extracted into the leachate. In terms of relative nutrient extraction efficiencies, the obtained results are in good agreement with results reported in the literature,[14,16−19,30] except for sodium, which was found lower in this work. There are several explanations for the difference in extraction efficiencies. The biomass samples used in the current study were subject to varying levels of drying in the field over winter, leading to a certain amount of nutrients being field-leached into the soil prior to collection. With some of the more readily leachable portions of nutrients already removed prior to the experiments, the extraction efficiency of the remaining nutrients would tend to be lower. Another reason for the discrepancy in removal efficiencies is the water/biomass ratios used in the literature, the residence times used, or a combination of both factors. The vast majority of researchers used very large water/biomass ratios, ranging from 15:1 to 120:1 (mg L^{-1}).[13,16−18,20] In combination with longer residence times ranging from 2 h to 2 days, this allowed for longer contact times and more water to interact with the biomass, leading to more leaching of nutrients. The moderate extraction of sodium could also be due to the low concentration of this element in the field-leached biomass; therefore, the reproducibility errors are not entirely unexpected.

Table 3 shows the miscanthus leachate element concentration at different leaching stages, as shown in Figure 1. The

Table 3. Concentration of Elements in Miscanthus Leachate (mg L^{-1}) at Different Leaching Stages[a]

elements	L1 (mg L^{-1})	L3 (mg L^{-1})	L4 (mg L^{-1})
sodium	8.7	31.2	63.9
calcium	17.6	52.0	73.2
potassium	142.3	391.3	650.8
magnesium	14.2	45.8	69.4
phosphorus	39.0	119.6	176.7
chloride	184.5	528.2	803.6
silica	9.5	25.3	
boron	ND[b]	ND	0.2
copper	ND	ND	0.5
iron	ND	ND	0.9
manganese	ND	ND	5.3
molybdenum	ND	ND	0.01
zinc	ND	ND	1.6
total solid	2473	8104	10654

[a]L2 was not tested for elemental analysis. [b]ND = not determined.

results obtained here show that the leachate nutrient concentration increases almost linearly with the number of stages, up to four stages. Element concentrations in leachate 4 were approximately 4 times higher than the concentrations in leachate 1 for most of the elements, such as calcium, potassium, magnesium, phosphorus, and chloride. Other components, such as boron, copper, iron, manganese, and zinc, were detected only in leachate 4 and not in leachates 1 and 3, because their concentrations were below the detection limit of the equipment. It is worth noting that the difference in the elemental concentration of L1 in Table 3 and miscanthus in Table 2 is due to the experimental error.

The results listed in Table 3 show that a multi-stage leaching process up to four stages does not decrease the nutrient extraction efficiency from biomass. It can also be concluded that the water consumption of an industrial leaching process is

dx.doi.org/10.1021/ef301452s | Energy Fuels 2012, 26, 7155−7163

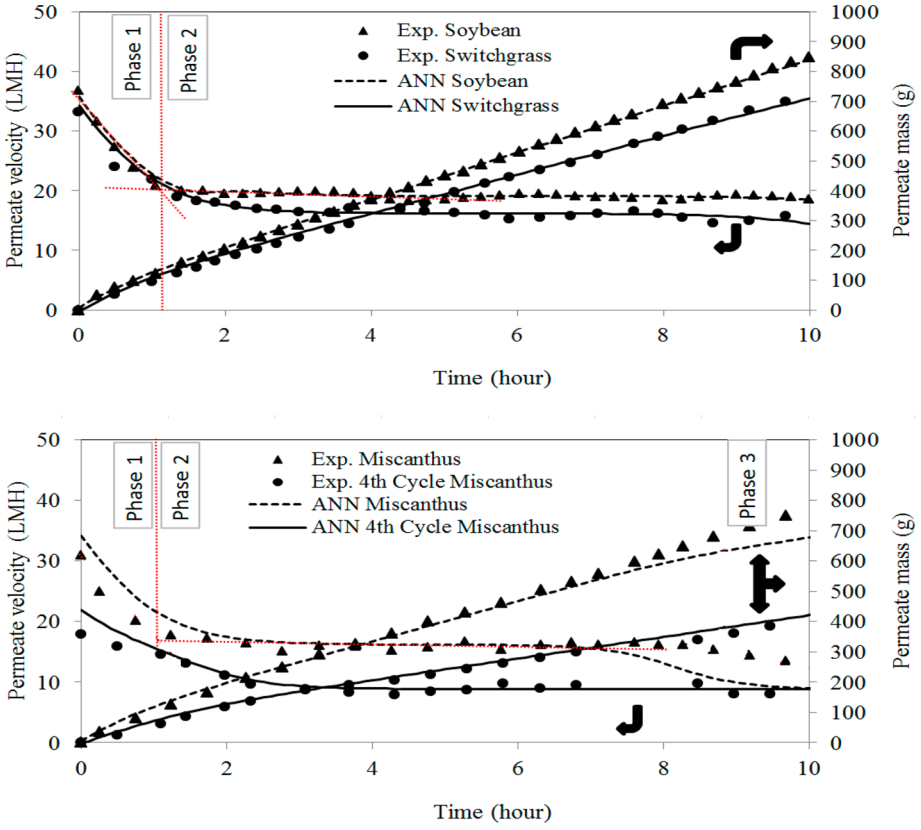

Figure 5. Permeate velocity [liters per square meter per hour (LMH)] and mass (g) versus time.

Table 4. Total Solid Concentration, Total Permeate, and Water Removal during 10 h of RO Filtration of Soybean (SB),[a] Switchgrass (SG),[a] Miscanthus (M),[b] and Miscanthus Fourth Cycle (M^{4th})[b]

	total solid concentration (mg/L)				total permeate (g)				water removal (%)			
time (h)	SB	SG	M	M^{fourth}	SB	SG	M	M^{fourth}	SB	SG	M	M^{fourth}
0	1740	2474	2587	10654	0	0	0	0	0	0	0	0
3	2005	2831	3452	12810	298	275	269	181	15	14	27	18
6	2312	3195	4714	14783	538	480	470	293	27	24	47	29
8	2567	3493	6163	16454	699	615	616	368	35	31	62	37
10	2909	3842	7859	18556	849	729	746	442	42	36	75	44

[a]Feed volume = 2 L. [b]Feed volume = 1 L.

significantly reduced through a multi-stage leaching process. Further optimization is recommended to determine the maximum number of cycles that are feasible.

4.2. RO. Permeate flux was measured during RO filtration of various biomass leachates under the operating transmembrane pressure of 1 MPa, and the results are shown in Figure 5. Permeate flux was calculated by differentiating the accumulated permeate mass with respect to time, divided by the permeate density and membrane surface area. Physical properties (e.g., density and viscosity) of the permeate were assumed to be constant and the same as those of water. The initial feed volumes for soybean and switchgrass leachates were 2 L. Two decline trends for the permeate flux were observed during RO filtration of soybean and switchgrass leachates. Permeate flux decreased sharply at the beginning of filtration, followed by a slight decline in the second phase. Permeate flux decreased by 46 and 33% for soybean and switchgrass from 37 and 33 L m^{-2} h^{-1} to 20 and 22 L m^{-2} h^{-1}, respectively, in the first hour of filtration. The primary reason for the permeate flux decline at the beginning of filtration is the formation of the concentration polarization layer on the membrane surface.[31] Concentration polarization is a result of solutes brought to the membrane by convective flux and their back transport to the bulk by diffusion. The thickness and concentration profile of the concentration polarization layer are controlled by the magnitude of the convection and diffusion terms.[32] Osmotic pressure arises as a result of the concentration polarization layer. Osmotic pressure lowers the permeate flux by decreasing the net driving potential needed to force the solvent to permeate through the membrane. The permeate flux decline was found to be less than 10% during the second phase of membrane fouling. The slight decrease in the permeate flux during the second phase was due to further deposition of particles on top of the first deposited layer. The water recovery values from the soybean and switchgrass leachates after 10 h of filtration were 42 and 36%, respectively (Table 4).

The lower permeate flux observed during the RO filtration of switchgrass leachate compared to the soybean permeate flux was mainly due to the higher total solid concentration of switchgrass leachate. The higher total solid concentration in the

dx.doi.org/10.1021/ef301452s | Energy Fuels 2012, 26, 7155−7163

leachate is translated to more solute accumulation on the membrane surface, leading to less permeate velocity.

The RO filtration of miscanthus and fourth cycle miscanthus leachates were carried out with 1 L of leachate. Three phases for reduction of permeate flux were experienced during the RO filtration of miscanthus leachate. Permeate flux decreased by 39% during the first hour filtration of miscanthus from 31 to 19 L m^{-2} h^{-1}. The second phase of permeate flux decline started after approximately 1 h of filtration and lasted for 7 h. Permeate flux remained almost constant during the second phase, followed by a sharper decrease after 8 h of filtration. The third phase may be due to further deposition of particles and/or consolidation of the fouling layer.[33] The third phase of permeate flux decline was observed only during the RO filtration of miscanthus, mainly because of the high water removal. Water removals from the miscanthus leachate after 8 and 10 h of filtration were 62 and 75%, respectively (Table 4). The total solid concentrations after 8 h of filtration of soybean, switchgrass, and miscanthus leachates were 2567, 3493, and 6163 mg L^{-1}, respectively. Permeate velocity of the fourth cycle miscanthus leachate was 9 L m^{-2} h^{-1} during the second phase of fouling. Permeate flux was lower during the RO filtration of fourth cycle miscanthus leachate because of the high total solid concentration, which resulted in high membrane fouling.

ICP testing was performed on the permeate for elemental analysis to calculate the solute rejections (eq 4). Figure 6 shows

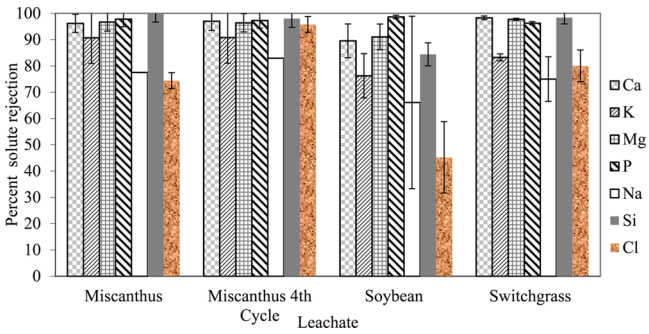

Figure 6. Percent solute rejections by membrane.

the result of this analysis. The amounts of calcium, magnesium, phosphorus, and silica showed rejection performance greater than 80% for all types of biomass leachate. Other elements with moderate rejections were potassium, sodium, and chlorine. Total solid rejection by the membrane was about 98% for all of the leachate samples.

4.3. Hybrid Neural Network Structure. Table 5 shows the performance of neural network models with various numbers of neurons in a single hidden layer. The performance of the network was tested by calculating R^2, mean absolute percent error, and maximum/minimum absolute percent errors for both training and testing phases. R^2 was found higher than 0.98 for neural networks with 4 and higher numbers of neurons. The mean percent absolute error decreased with an increasing the number of neurons from 2 to 6. Increasing the number of neurons from 2 to 4 lowered the mean absolute percent error of the whole data set (training and testing data sets) by approximately 76%. Increasing the number of neurons from 4 to 6 decreased the mean absolute percent error only by 12%. The mean absolute percent error of approximately 3% was found for the networks with 4 and 5 neurons. To prevent overtraining of the ANN model, 4 neurons in one hidden layer was selected as the optimum value for the ANN structure. Employing this configuration, the permeate flux was predicted with a maximum percent absolute error of 14%.

Figure 7 shows the scatter plots of the predicted (ANN) permeate flux versus the experimental data (left panel) and the percent error for the training and testing data points. The developed ANN model (2:4:1) was capable of predicting permeate flux with a mean absolute percent error of approximately 3% for both training and testing phases. The scatter plot of percent error versus total solid concentration and filtration time followed no specific trend.

The mathematical algorithm in Figure 4 was used to predict the permeate flux during the RO filtration of biomass leachates. The input variables to this algorithm were the initial feed volume, the total solid concentration, the membrane effective surface area, and the membrane rejection coefficient. The trained ANN (2:4:1) model was used in the algorithm. The total solid concentration and filtration time were the inputs of the ANN model for the estimation of the permeate velocity. The total solid concentration in the feed tank and feed volume at each time step were calculated by integrating eqs 2 and 5 and were updated at each time step. The rejection coefficient of the total solid concentration was assumed to be constant during the RO filtration of the biomass leachate. The algorithm continued until the desired filtration time was reached. Figure 5 compares the permeate velocity obtained from the algorithm (proposed in Figure 4) to the experimental data. Good agreement was observed between the predicted results and experimental data. A slight deviation from the experimental data was observed for the permeate flux during the RO filtration of miscanthus leachate. The time steps of Δt should be considered small enough to capture the sharp permeate flux decrease at the beginning of the filtration. Different sizes for the time step were tested, and a value of 1×10^{-2} h was selected. It was found that the permeate flux was independent of the time step for the intervals less than this particular value.

Table 5. Performance of ANN with Various Numbers of Neurons in One Hidden Layer

	training data set				testing data set				validation data set	
network	R^2	maximum absolute percent error (%)	minimum absolute percent error (%)	mean absolute percent error (%)	R^2	maximum absolute percent error (%)	minimum absolute percent error (%)	mean absolute percent error (%)	maximum absolute percent error (%)	mean absolute percent error (%)
(2:2:1)	0.76	39.21	0.51	13.17	0.88	28.58	0.69	9.15	20.5	15.5
(2:3:1)	0.96	18.87	0.08	4.74	0.94	14.59	0.37	7.07	57.3	15.5
(2:4:1)	0.98	14.48	0.03	3.07	0.98	10.26	0.22	3.06	24.1	14.7
(2:5:1)	0.99	12.63	0.00	3.04	0.99	8.27	0.82	3.36	275.6	93.1
(2:6:1)	0.99	10.66	0.00	2.65	0.99	6.42	0.05	2.72	77.6	21.8

dx.doi.org/10.1021/ef301452s | Energy Fuels 2012, 26, 7155−7163

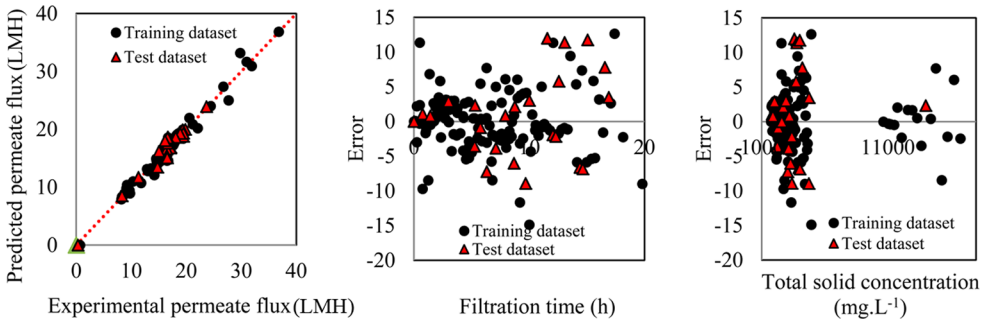

Figure 7. (Left panel) Predicted versus experimental permeate flux, (middle panel) percent error versus filtration time, and (right panel) percent error versus total solid concentration, using ANN (2:4:1).

The mathematical model was validated against unseen experimental permeate flux data. The model results were validated against experimental data obtained from a 20 h RO filtration of soybean leachate, as summarized in Tables 5 and 6.

Table 6. Predicted and Experimental Permeate Flux for 36 h of RO Filtration of Soybean Leachate

time (h)	total solid concentration (mg L^{-1})	percent water removed (%)	experimental permeate flux (LMH)	predicted permeate flux (LMH)
0.1	1746	1	36.8	35.7
3	2005	15	19.9	19.5
6	2312	27	19.5	19.1
9	2733	39	19.4	18.9
12	3303	50	16.8	15.1
15	3908	58	14.9	11.9
18	4399	65	10.4	11.8
21	5667	72	NA	8.9
24	6965	77	NA	8.9
27	9070	83	NA	8.9
30	13093	88	NA	8.9
35	55955	98	NA	8.9

A mean absolute percent error of 15% was observed for the ANN with 4 neurons in the hidden layer. A steady-state permeate flux of 8.9 L m^{-2} h^{-1} was achieved after approximately 19 h of filtration when 69% of water was removed from the soybean leachate. The mathematical model estimated that it takes 35 and 36 h to recover 98 and 99% of water from the soybean leachate using the current RO filtration module, respectively.

5. CONCLUSION

Potential implementation of RO to recover nutrients from three types of biomass leachate and the improvement in the combustion properties of the biomass were studied in this paper using a laboratory investigation and a hybrid ANN modeling scheme. Results obtained from the study help to better understand the permeate flux behavior and determine the amount of nutrients recovered from the biomass leachate using RO filtration. The following conclusions can be drawn on the basis of the results obtained from the present study: (1) Combustion properties of biomass were improved by extracting water-soluble nutrients. Chlorine and potassium were the most leachable nutrients in biomass. Approximately 100 and 89% of chlorine in miscanthus and soybean were extracted into the leachate. The extraction efficiency of potassium was more than 50%. Other elements with moderate extraction efficiencies were magnesium, phosphorus, sodium, and to a lesser extent, calcium. The nutrient extraction efficiencies were in good agreement with the results reported in the literature, except for sodium, which was found lower in this work. (2) The results obtained in this work showed that a multi-cycle leaching process of up to four stages did not decrease the nutrient extraction efficiency from biomass. This represents an improvement to the process when applied on an industrial scale. The ability to recycle the leachate reduces the amount of fresh water required for the overall process. (3) RO was found to be an efficient technique to recover nutrients from biomass leachate. Over 80% of calcium, magnesium, phosphorus, and silica were recovered by the RO membrane, which was in agreement with the literature data. For future research, it is recommended to use a spiral-wound membrane module to further study and optimize the RO process implemented for the water recovery and nutrient concentration from biomass leachate. Spiral membranes are high performing and incorporate a significantly larger membrane area than the flat sheet membranes. (4) Permeate flux was high at the beginning of the filtration, depending upon the initial total solid concentration of leachate. Permeate flux decreased sharply at the beginning of the filtration followed by a slight decline during the course of filtration. (5) An intelligent model based on the feed-forward ANN coupled with membrane mathematical equations was used to predict the permeate flux during the filtration. The optimum network configuration is 2 input neurons, 4 hidden neurons, and 1 output neuron (2:4:1). Having the optimal network, the maximum absolute error percentage was about 14%. The hybrid ANN model was validated against the experimental data, showing acceptable agreement.

AUTHOR INFORMATION

Corresponding Author

*E-mail: arrajabz@uwaterloo.ca.

Notes

The authors declare no competing financial interest.

ACKNOWLEDGMENTS

Investment in this project has been provided by Agriculture and Agri-Food Canada through the Canadian Agricultural Adaptation Program (CAAP). In Ontario, this program is delivered by the Agricultural Adaptation Council. The authors also thank Jabeen Waheed and Mindy Cleave for assisting with the lab experiments.

NOMENCLATURE

Acronyms

ANN = artificial neural network
BP = back propagation
ICP−OES = inductively coupled plasma−optical emission spectrometry
RO = reverse osmosis
TDS = total dissolved solids
LMH = liters per square meter per hour

Variables

A = effective membrane surface area (m^2)
C_F = feed total solid concentration (mg L^{-1})
C_P = permeate total solid concentration (mg L^{-1})
J = permeate flux (L m^{-2} h^{-1})
Q_P = permeate volumetric flow rate (m^3 h^{-1})
R = rejection coefficient
R'' = percent removal of nutrients in biomass
t = filtration time (h)
T = temperature (°C)
V_F = feed volume (m^3)
X = normalized value of variable x
x_{max} = highest value of variable x
x_{min} = lowest value of variable x

REFERENCES

(1) United States Energy Information Administration (EIA). *International Energy Outlook 2011*; EIA: Washington, D.C., 2012; EIA-DOE-0484.
(2) Jenkins, B. M.; Bakker, R. R.; Wei, J. B. *Biomass Bioenergy* **1996**, *10*, 177−200.
(3) Larsen, O. H.; Montgomery, M. *Energy Mater.* **2006**, *1*, 227−237.
(4) Mettanant, V.; Basu, P.; Butler, J. *Can. J. Chem. Eng.* **2009**, *87*, 656−684.
(5) Miles, T. R.; Miles, T. R., Jr.; Baxter, L. L.; Bryers, R. W.; Jenkins, B. M.; Oden, L. L. *Biomass Bioenergy* **1996**, *10*, 125−138.
(6) Steenari, B.; Lundberg, A.; Pettersson, H.; Wilewska-Bien, M.; Andersson, D. *Energy Fuels* **2009**, *23*, 5655−5662.
(7) Ogden, C. A.; Ileleji, K. E.; Johnson, K. D.; Wang, Q. *Fuel Process. Technol.* **2010**, *91*, 266−271.
(8) Robinson, A. L.; Junker, H.; Baxter, L. L. *Energy Fuels* **2002**, *16*, 343−355.
(9) Turn, S. Q.; Kinoshita, C. M.; Ishimura, D. M.; Zhou, J. *Fuel* **1998**, *77*, 135−146.
(10) Jenkins, B. M.; Mannapperuma, J. D.; Bakker, R. R. *Fuel Process. Technol.* **2003**, *81*, 223−246.
(11) Thy, P.; Jenkins, B. M.; Williams, R. B.; Lesher, C. E.; Bakker, R. R. *Fuel Process. Technol.* **2010**, *91*, 1464−1485.
(12) Turn, S. Q.; Kinoshita, C. M.; Jakeway, L. A.; Jenkins, B. M.; Baxter, L. L.; Wu, B. C.; Blevins, L. G. *Fuel Process. Technol.* **2003**, *81*, 35−55.
(13) Vamvuka, D.; Zografos, D.; Alevizos, G. *Bioresour. Technol.* **2008**, *99*, 3534−3544.
(14) Yu, C.; Zheng, Y.; Cheng, Y.; Jenkins, B. M.; Zhang, R.; VanderGheynst, J. S. *Bioresour. Technol.* **2010**, *101*, 4331−4336.
(15) Khan, A. A.; de Jong, W.; Jansens, P. J.; Spliethoff, H. *Fuel Process. Technol.* **2009**, *90*, 21−50.
(16) Arvelakis, S.; Gehrmann, H.; Beckmann, M.; Koukios, E. G. *Fuel* **2003**, *82*, 1261−1270.
(17) Arvelakis, S.; Gehrmann, H.; Beckmann, M.; Koukios, E. G. *Biomass Bioenergy* **2005**, *28*, 331−338.
(18) Giuntoli, J.; Arvelakis, S.; Spliethoff, H.; de Jong, W.; Verkooijen, A. *Energy Fuels* **2009**, *23*, 5695−5706.
(19) Arvelakis, S.; Koukios, E. G. *Biomass Bioenergy* **2002**, *22*, 331−348.
(20) Vamvuka, D.; Zografos, D. *Fuel* **2004**, *83*, 2051−2057.
(21) Blanco-Canqui, H.; Lal, R. *Crit. Rev. Plant Sci.* **2009**, *28*, 139−163.
(22) Kucera, J. *Reverse Osmosis: Design, Processes and Applications for Engineers*; Wiley: Hoboken, NJ, 2010.
(23) Van Voorthuizen, E. M.; Zwijnenburg, A.; Wessling, M. *Water Res.* **2005**, *39*, 3657−3667.
(24) Bilstad, T. *J. Membr. Sci.* **1995**, *102*, 93−102.
(25) Colyar, K. R. M.S. Thesis, University of Colorado, Boulder, CO, 2008.
(26) Torrecilla, J. S.; Otero, L.; Sanz, P. D. *J. Food Eng.* **2005**, *69*, 299−306.
(27) Alshihri, M. M.; Azmy, A. M.; El-Bisy, M. *Constr. Build. Mater.* **2009**, *23*, 2214−2219.
(28) Hagan, M. T. *Neural Network Design*; PWS Pub.: Boston, MA, 1996.
(29) Tambe, S. S.; Kulkarni, B. D.; Deshpande, P. B. *Elements of Artificial Neural Networks with Selected Applications in Chemical Engineering, and Chemical and Biological Sciences*; Simulations and Advanced Control, Ltd.: Louisville, KY, 1996.
(30) Piotrowska, P.; Zevenhoven, M.; Hupa, M.; Giuntoli, J.; de Jong, W. *Fuel Process. Technol.* **2013**, *105*, 37−45.
(31) Marshall, A. D.; Munro, P. A.; Tragardh, G. *Desalination* **1993**, *91*, 65−108.
(32) Rajabzadeh, A. R.; Moresoli, C.; Marcos, B. *J. Membr. Sci.* **2010**, *361*, 191−205.
(33) Turker, M.; Hubble, J. *J. Membr. Sci.* **1987**, *34*, 269−281.